Bioorthogonal Reactions

DOI: 10.1002/ange.201305969

Click to Release: Instantaneous Doxorubicin Elimination upon Tetrazine Ligation**

*Ron M. Versteegen, Raffaella Rossin, Wolter ten Hoeve, Henk M. Janssen, and Marc S. Robillard**

Bioorthogonal conjugation or click reactions are enjoying widespread use in the fields of chemistry, chemical biology, molecular diagnostics, and medicine, among others, where they enable the selective manipulation of molecules, cells, particles and surfaces, and the tagging and tracking of biomolecules in vitro and in vivo.[1] These reactions include the Staudinger ligation, the azide–cyclooctyne cycloaddition, and the inverse-electron-demand Diels–Alder (inv-DA) reaction.[1,2] Analogous to click reactions, cleavable linkers, such as the redox-sensitive disulfide and diazo linkers and the hydrazine-labile levulinoyl linker, have many potential uses in biological media.[3] Although these linkers are selective, they often lack the level of bioorthogonality and broad applicability of the click reactions, which is especially relevant when extending the application scope to living cells, animals, and humans. This issue may be addressed by adapting a click reaction to effect selective release, instead of, or in addition to, selective conjugation. From this family of reactions, only the Staudinger ligation[4] and the parent Staudinger reaction[5] have been applied in selective cleavage. However, their reactivity is low, and the phosphine reagents are prone to oxidation. We set out to develop a new bioorthogonal and rapid elimination reaction that in addition to a broad scope of in vitro applications would allow effective chemical manipulation in living systems, and eventually humans. One potential application is antibody–drug-conjugate (ADC) release, wherein the linker between the tumor-bound antibody and the drug is selectively cleaved through reaction with a probe, which is administered in a second step. This approach does not rely on the currently employed endogenous intracellular ADC activation mechanisms (such as enzymatic activation), and thus expands the scope of suitable ADC targets to those that do not efficiently internalize and to extracellular-matrix constituents.[6]

So far, only the fastest click reaction, the inv-DA reaction, has shown sufficient potential for use in living systems under clinically relevant conditions. In the context of tumor-pretargeted radioimmunoimaging, we[7,8] and others[9,10] have shown that the inv-DA reaction between antibody-conjugated *trans*-cyclooctene (TCO) and a radiolabeled tetrazine occurs effectively in mice at low equimolar concentrations (Figure 1 a and Scheme 1 a). The cycloaddition results in an intermediate that rearranges by expulsion of dinitrogen in a retro-Diels–Alder cycloaddition to a 4,5-dihydropyridazine **5**, which may tautomerize to a 1,4-dihydropyridazine **6**,[2,11,12] especially under aqueous conditions.[13] Depending on the substituents, the dihydropyridazine can be converted into an aromatic pyridazine **7** in the presence of an oxidant, such as dioxygen.[12] Importantly, the conversion of dihydropyridazines into a pyridazine by the elimination of a leaving group from the vinyl position or through a double-bond shift has also been shown.[12,14]

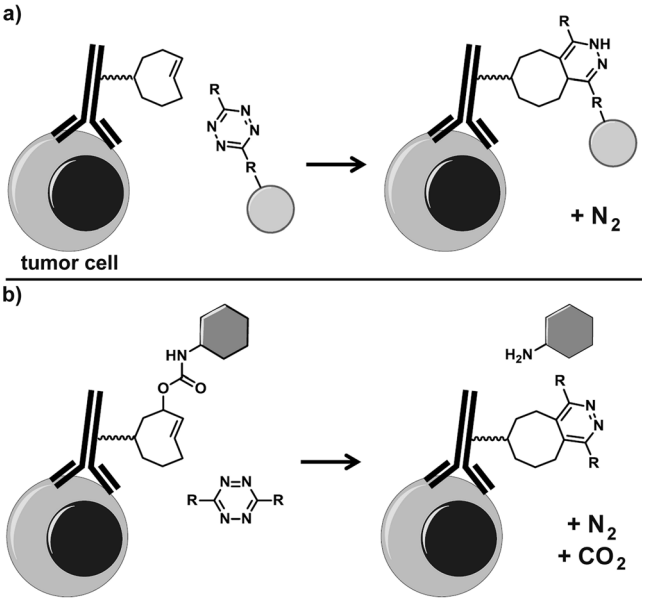

Figure 1. a) Tumor pretargeting with the inverse-electron-demand Diels–Alder (inv-DA) cycloaddition in live mice (circle: radiolabeled moiety).[7] b) Envisioned on-tumor antibody–drug-conjugate (ADC) release and activation enabled by the new inv-DA-based elimination reaction (hexagon: drug).

We consequently envisioned that the versatile dihydropyridazine motif could be enlisted to provoke the release of

[*] R. Rossin, M. S. Robillard
Tagworks Pharmaceuticals
High Tech Campus 11, 5656 AE Eindhoven (The Netherlands)
E-mail: marc.robillard@tagworkspharma.com
R. M. Versteegen, H. M. Janssen
SyMO-Chem
Den Dolech 2, 5612 AZ Eindhoven (The Netherlands)
W. ten Hoeve
Syncom
Kadijk 3, 9747 AT Groningen (The Netherlands)

[**] We thank L. H. J. Kleijn (SyMO-Chem) for assistance in synthesis of the starting compounds, Dr. Johan Lub for insightful discussions, and Hugo Knobel for HRMS measurements (Philips Research). This research is supported by NanoNextNL (The Netherlands).

Supporting information for this article is available on the WWW under http://dx.doi.org/10.1002/anie.201305969.

a suitably positioned TCO-bound substance, such as a drug (Figure 1b and Scheme 1b). In particular, we hypothesized that the 1,4-dihydropyridazine product **10** derived from a tetrazine and a TCO **8** containing a carbamate-linked drug at the allylic position could be prone to undergo conversion into a conjugated pyridazine **11** by the formation of an exocyclic double bond with the elimination of CO_2 and an NH_2-substituted drug **14**. The pyridazine **11** might subsequently rearrange to the favored aromatic pyridazine **12**. The key features of **10** resemble those of the well-established self-immolative *p*-aminobenzyloxycarbonyl (PABC) linker used in ADCs;[15] in a similar fashion, the shift of the electron lone pair of NH into the ring may enable an electronic-cascade-based release of the drug (Scheme 1b). We also considered the less likely possibility that **14** could be expelled from the 4,5-tautomer **9** by carbamic acid elimination (decarboxylation) initiated by removal of the H-4 proton, again to afford **11**; analogously, **14** could be expelled from **13**. Such a process is similar to that observed with β-eliminative linkers used in drug-linked macromolecules and hydrogels, but would require a sufficiently acidic H-4 atom.[16]

To test our hypothesis, we prepared model compounds (*E*)-cyclooct-2-en-1-yl benzylamine carbamate (**8a**,**e-Bn**) and the doxorubicin conjugates (*E*)-cyclooct-2-en-1-yl doxorubicin carbamate (**8a**,**e-Dox**; Scheme 1b–d). The anticancer drug doxorubicin was selected as a model for future ADC applications with potent toxins. (*Z*)-Cyclooct-2-enol (**15**) was isomerized to (*E*)-cyclooct-2-enol (**16**) by photolysis[17] to afford two isomers with the hydroxy group positioned either axially (isomer **16a**) or equatorially (isomer **16e**).[18] (*E*)-Cyclooct-2-enol (**16**) was subsequently converted with benzylisocyanate or doxorubicin (via 4-nitrophenylcarbonate activation of **16**) into compounds **8** (Scheme 1). We also prepared three tetrazines spanning a wide range in electron density: 3,6-bis(2-pyridyl)-1,2,4,5-tetrazine (**2**), 3-(2-pyridyl)-6-methyl-1,2,4,5-tetrazine (**3**), and 3,6-dimethyl-1,2,4,5-tetrazine (**4**), which were stable in phosphate-buffered saline

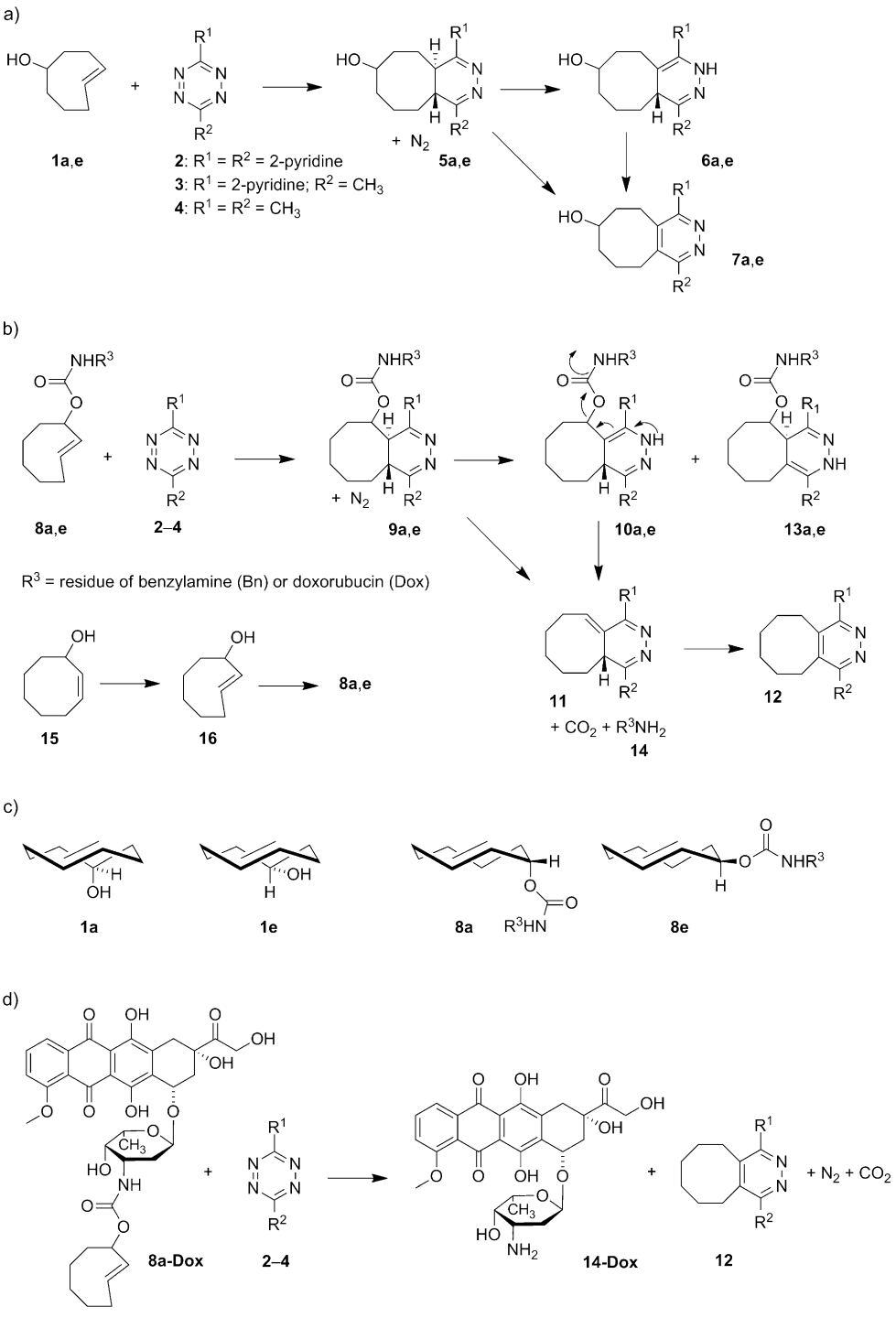

Scheme 1. a) Inv-DA reaction between TCO **1** and tetrazines **2**–**4**. b) Synthesis of TCO **8** and potential release mechanisms from inv-DA product **9**, following the reaction of **8** with tetrazines **2**–**4**; not all possible tautomer conversions and stereoisomers are shown. c) Equatorial and axial isomers of (*E*)-cyclooct-4-enol **1** and (*E*)-cyclooct-2-en-1-yl carbamates **8**. d) Doxorubicin (**14-Dox**) release from TCO conjugate **8a-Dox.** **a**: axially substituted *trans*-cyclooctene; **e**: equatorially substituted *trans*-cyclooctene.

Table 1: Tetrazine stability and reactivity (second-order rate constants) towards TCO constructs, as measured by UV/Vis spectroscopy at 540 nm ($n=3$).

Probe	Tetrazine stability at 37 °C		Tetrazine reactivity with TCOs in MeCN at 20 °C: k_2 [$M^{-1}s^{-1}$]		
	in PBS: $t_{1/2}$ [h]	in serum: proportion intact at 4 h [%]	**8e-Bn**	**8a-Bn**	**1a**
2	9.6 ± 0.13	75.1 ± 4.2	0.37 ± 0.10	57.7 ± 5.0	1140 ± 85
3	141.5 ± 14.80	96.3 ± 1.9	–	5.94 ± 0.24	–
4	14.4 ± 0.35	100 ± 2.0	–	0.54 ± 0.06	–

(PBS) at 37 °C with half-lives greater than 9 h (Table 1). The reactivity of **2** towards the reference TCO (*E*)-cyclooct-4-enol **1a** (Scheme 1a,c) was 1140 $M^{-1}s^{-1}$ in MeCN at 20 °C, which corresponds to at least the rate constant of $k_2 = 7.9 \times 10^4\ M^{-1}s^{-1}$ in water at 20 °C found for **1a** and a slightly less reactive 4-amido-2-pyridyl derivative of **2**.[8] The reactivity of **2** towards axial and equatorial **8a**,**e-Bn** was 57.70 and 0.37 $M^{-1}s^{-1}$, respectively, in MeCN at 20 °C (Table 1). Although the axial isomer would be expected to be more reactive,[8] the large 156-fold difference is probably also due to steric hindrance of the approach of the tetrazine by the equatorial benzylcarbamate moiety. The 20-fold lower reactivity of **8a-Bn** as compared to that of **1a** is presumably a result of the same steric effect. We selected **8a-Bn** for subsequent studies, measured its reactivity with tetrazines **3** and **4**, and found an expected approximately 10- and 100-fold decrease relative to its reactivity with **2** owing to the increased electron density in these tetrazines (Table 1). Carbamate **8a-Bn** appeared to be as stable ($t_{1/2} \geqslant 20$ days in PBS at 20 °C) as the (*E*)-cyclooct-4-enol-derived carbamates that are widely used in click reactions.[1,2]

We next used ^{1}H NMR spectroscopy to monitor the reaction between TCO **8a-Bn** and tetrazine **4** in dry [D_3]MeCN at 20 °C. Within minutes, a rapid inv-DA reaction led to the complete conversion of tetrazine **4** and the formation of the initial 4,5-tautomer of the inv-DA adduct (**9a**,Figure 2; see also Figure S3 in the Supporting Information). To our delight, the amount of the 4,5-tautomer started to decline after approximately 10 min in conjunction with the formation of free benzylamine (**14-Bn**) and the non-aromatic elimination product **11**, characterized by the alkylidene proton at 6.55 ppm. Intermediate **11** spontaneously rearranged to aromatic **12**, the signals for which matched the characteristic signals of a similar (*E*)-cyclooctene-derived 3,6-diphenyl-pyridazine reported by Fox and coworkers.[13] In parallel, the initial 4,5-tautomer was converted into a product with equal mass, according to GC–MS (see Figure S5) and HPLC–MS/PDA (PDA = photodiode array; Figure 3a). This product was identified as the 1,4-tautomer **10a/13a** on the basis, for example, of the D_2O-exchangeable NH signal at $\delta = 7.05$ ppm (see Section S6 in the Supporting Information).[19] Overall, the reaction yielded about 60% of both benzylamine (**14-Bn**) and the elimination product **12**, and 40% of the 1,4-tautomer **10a/13a**, which did not eliminate benzylamine (Figure 3a; see Figure S4 for a plot of product formation for this NMR spectroscopic experiment). When the reaction was repeated in 33% [D_3]MeCN in deuterated PBS, we observed an expected faster reaction and 64% free benzylamine, thus demonstrating maintained efficacy of the pyridazine elimination under aqueous conditions (see Section S6 in the Supporting Information).

In contrast to the reaction with **4**, no significant release of benzylamine was observed for the reaction of **8a-Bn** with **2** in dry [D_3]MeCN or in 33% [D_3]MeCN in deuterated PBS after 18 h. ^{1}H NMR spectroscopic analysis in [D_3]MeCN did reveal the rapid formation of the 4,5-tautomer of the inv-DA adduct, but this structure appeared to be stable. The results of the reaction between **8a-Bn** and tetrazine **3** fell in between those of the reactions of **2** and **4**, with 45% benzylamine released after 18 h in 33% [D_3]MeCN in deuterated PBS. Despite the complexity arising from the unsymmetrically substituted tetrazine **3** and the corresponding regioisomers of the inv-

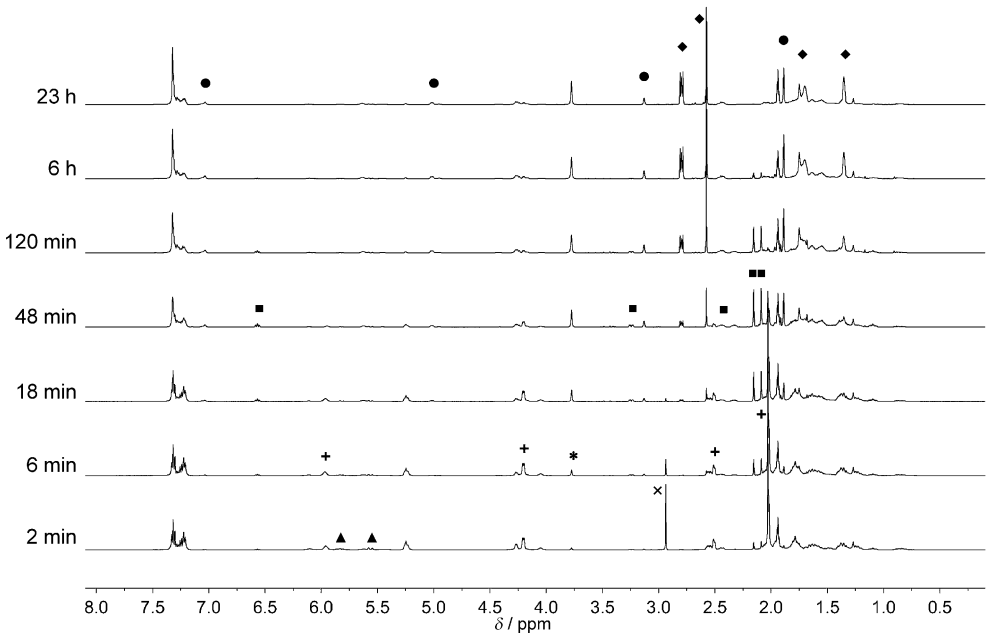

Figure 2. ^{1}H NMR spectroscopic analysis of the reaction of tetrazine **4** with TCO **8a-Bn** in [D_3]MeCN at 20 °C. Legend: ×: tetrazine **4**; ▲: TCO **8a-Bn**; +: 4,5-inv-DA adduct **9a** (R^1,$R^2 = CH_3$; R^3 = Bn); ■: non-aromatic elimination product **11**; ◆: aromatic elimination product **12**; ●: 1,4-inv-DA adducts **10a/13a** (R^1,$R^2 = CH_3$; R^3 = Bn); ⋆: benzylamine (**14-Bn**).

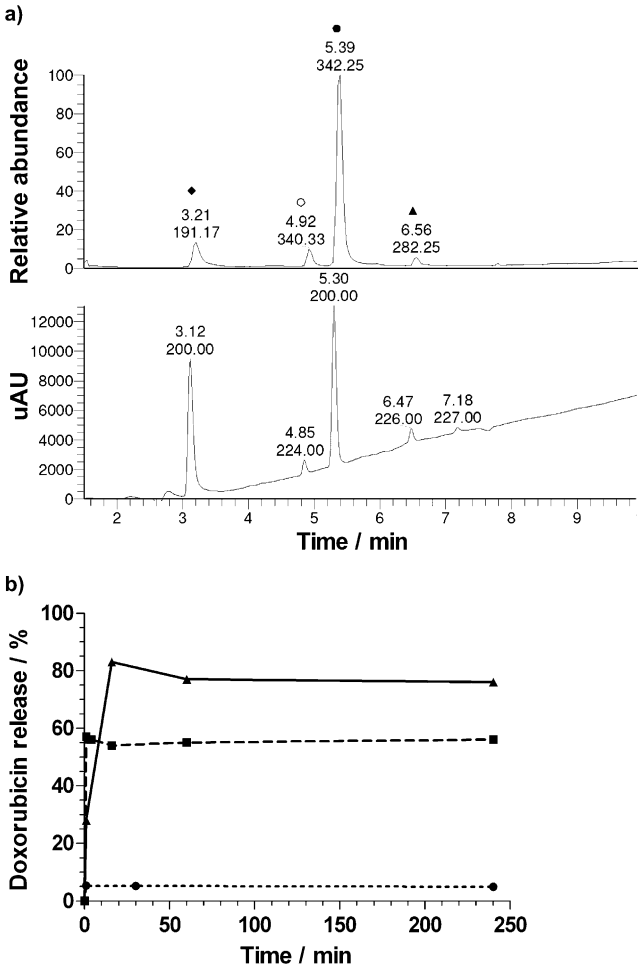

Figure 3. a) HPLC–MS/PDA analysis of the reaction of tetrazine **4** with TCO **8a-Bn** in [D_3]MeCN at 20°C after 18 h. The upper graph is the MS trace in the positive mode; the lower graph is the PDA trace. Legend: ◆: elimination product **12**; ●: inv-DA adduct **10a/13a** (R^1,R^2 = CH_3; R^3 = Bn); ▲: excess TCO **8a-Bn**; ○: oxidized inv-DA adduct (possibly formed during analysis); **14-Bn** is not visible. b) Doxorubicin (**14-Dox**) release (%) from **8a-Dox** following the addition of tetrazine **2**–**4** (10 equiv) in 25% MeCN in PBS as measured by HPLC–MS/PDA. Legend: dotted line: **2**; dashed line: **3**; solid line: **4**.

DA product, key ^{1}H NMR signals in dry [D_3]MeCN, such as the triplet for the alkylidene hydrogen atom of **11** at δ = 6.75 ppm, were similar to those observed for the reaction of **4** (see Figure S3 and Section S6 in the Supporting Information).

The inv-DA reaction and the subsequent cleavage of the carbamate can give rise to multiple interconverting tautomers and stereoisomers, the relative abundances of which are probably dependent on the tetrazine substituents R^1 and R^2 and the reaction medium, among other factors. Therefore, further work is required to fully elucidate the elimination pathway. Nevertheless, the elimination has been shown to occur via **9**, to depend on the nature (e.g. electron density) of the tetrazine, and to lead to the key intermediate **11**, thus supporting the hypothesis that it is driven by the inv-DA reaction and dihydropyridazine rearrangement. It is known that 4,5- to 1,4-tautomerization may occur readily under water-free conditions by virtue of a 1,3-hydride shift,[11,12] and therefore it is possible that **9** leads to a short-lived intermediate **10**, which liberates **14**, whereas formed **13** does not release this moiety. However, the results so far also support direct elimination from **9** to **11** (or similarly from **13**), whereby **10** cannot liberate **14**. Importantly, from the product-formation plot it follows that aromatization to **12** cannot be the driver of the elimination, as it occurs on a longer time scale than the formation of **14** (see Figure S4 in the Supporting Information).

We subsequently employed HPLC–MS/PDA to study the release of doxorubicin (**14-Dox**) from the TCO conjugate **8a-Dox** (25 μM) as induced by **2**–**4** (10 equiv) in 25% MeCN in PBS at 37°C (Table 2 and Figure 3b; see also Figure S6). The

Table 2: Doxorubicin (**14-Dox**) release from **8a-Dox** following the addition of tetrazine **2**–**4** (10 equiv) in 25% MeCN in PBS or 50% serum at 37°C, as measured by HPLC–MS/PDA at 4 h (n = 3).

Probe	Doxorubicin release [%] in PBS/MeCN (3:1)	in serum
2	7 ± 3	12 ± 1
3	55 ± 4	46 ± 3
4	79 ± 3	75 ± 4
–[a]	0	0

[a] No release of **14-Dox** from **8a-Dox** was observed at 37°C in PBS (72 h) or serum (24 h).

reactions were complete within minutes and, in analogy to the NMR spectroscopic experiments, treatment with **2** gave almost no **14-Dox** (7%), whereas **3** and **4** afforded free **14-Dox** in 55 and 79% yield, respectively, after 4 h (Table 2). In fact, the elimination reached its maximum within 4 min for **3** and 16 min for **4** (limited by its lower reactivity; Figure 3b). Analogous to **8a-Bn**, the reaction between **8a-Dox** and tetrazines **2**–**4** afforded dihydropyridazine products that either led to rapid doxorubicin release or remained stable. No evidence was found by MS for the deactivation of **9**, **10**, or **13** by oxidative aromatization. To determine whether the elimination is dependent on the TCO isomer, we monitored the reaction between **8e-Dox** and **3** in PBS at 37°C and found a similar value for liberated **14-Dox** (51 ± 1.5%; n = 3) after 4 h. Next, we tested the release from **8a-Dox** in serum with tetrazines **2**–**4** (largely stable in serum for 4 h; Table 1) and found similar values to those obtained in PBS (Table 2). This finding and the fact that **8a-Dox** by itself did not liberate **14-Dox** for at least 24 h in PBS or serum at 37°C support the bioorthogonality of the system. The faster elimination observed in the HPLC experiments in 25% MeCN in PBS as compared to the NMR experiments in [D_3]MeCN indicates an important role of water in the release and possibly supports the mechanism involving the conversion of **10** into **11**. The slightly higher yields relative to those observed in the NMR experiments in 33% [D_3]MeCN in PBS are possibly due to the increased percentage of water and/or the increased temperature. The formic acid used in HPLC–MS/PDA was shown by NMR spectroscopy to facilitate the aromatization

of **11** to give **12**, but not the formation of benzylamine (**14-Bn**) from **8a-Bn** (data not shown).

Finally, having established the proof of principle of the inv-DA pyridazine elimination, we were interested in testing the system in a cellular environment. Although future efforts will be focused on applying the system in ADCs, we expected that unconjugated **8a-Dox** would still have a lower cytotoxicity than that of the parent **14-Dox**, possibly also owing to differences in cellular uptake, thus allowing the monitoring of its activation in an in vitro cytotoxicity assay.[5] Indeed, when tetrazines **2**–**4** (10 μM) were combined with the TCO conjugate **8a-Dox** in an A431 cell culture, increased cytotoxicity by a factor of 14, 53, and 78 (EC_{50}: 0.280, 0.072 and 0.049 μM), respectively, was observed relative to that of **8a-Dox** alone (EC_{50}: 3.834 μM). These values reflect the different maximal release percentages and the EC_{50} value of 0.037 μM of **14-Dox** alone (Scheme 1d and Table 3; see also Figure S7). This effective recovery of the cytotoxicity of the parent drug, combined with the higher EC_{50} values found for tetrazines **2**–**4** alone, indicates that **8a-Dox** was efficiently activated.

Table 3: EC_{50} (half-maximal effective concentration) values for doxorubicin (**14-Dox**), tetrazines **2**–**4**, and the TCO conjugate **8a-Dox** alone and in the presence of tetrazines **2**–**4**, as obtained from proliferation assays on A431 tumor cells.

Compound	EC_{50} [μM][a]
14-Dox	0.037 (0.026–0.052)
8a-Dox	3.834 (2.051–7.166)
8a-Dox + **2** (10 μM)	0.280 (0.208–0.375)
8a-Dox + **3** (10 μM)	0.072 (0.053–0.097)
8a-Dox + **4** (10 μM)	0.049 (0.036–0.066)
2	18.98 (11.99–30.04)
3	21.05 (12.22–36.24)
4	48.23 (27.28–85.24)

[a] The EC_{50} 95% confidence interval ($n = 3$) is given in parentheses.

In summary, we have developed a new bioorthogonal elimination reaction that enables instantaneous, self-immolative, and traceless release of a substance from *trans*-cyclooctene following tetrazine ligation. In this proof-of-principle study, the inv-DA pyridazine elimination reached 79% yield within minutes under ambient conditions at micromolar concentrations. The components are essentially the same as those used successfully in living systems, and we expect that further optimization of the reactivity and release will lead to application as a novel chemically cleavable ADC linker.[20] Identification of the drug-releasing tautomer is key, as this may provide inroads to new inv-DA components that will favor its formation. The *trans*-cyclooct-2-enol building block is readily accessible, and ample options exist for the preparation of bifunctional derivatives for conjugation. The use of a radiolabeled tetrazine as the drug-releasing probe would possibly allow a combination of the ADC approach with pretargeted radioimaging or radiotherapy to monitor drug release or for combination therapy, respectively. Besides ADC applications, we also envision the use of inv-DA-cleavable linkers or masking moieties in bi- and trispecific biologics, chemical biology, life-science assays, and materials chemistry to enable the controlled (dis)assembly of molecules, proteins, cells, or biomaterials. The availability of an elimination reaction with the bioorthogonality and speed of the inv-DA will enable enhanced control over chemical and biological manipulations in vitro and in living systems.

Received: July 9, 2013
Revised: October 15, 2013
Published online: November 26, 2013

Keywords: cycloaddition · *trans*-cyclooctene · elimination · pyridazines · tetrazines

[1] M. Debets, J. C. M. van Hest, F. P. J. T. Rutjes, *Org. Biomol. Chem.* **2013**, *11*, 6439–6455.
[2] M. L. Blackman, M. Royzen, J. M. Fox, *J. Am. Chem. Soc.* **2008**, *130*, 13518–13519.
[3] G. C. Rudolf, W. Heydenreuter, S. A. Sieber, *Curr. Opin. Chem. Biol.* **2013**, *17*, 110–117.
[4] M. Azoulay, G. Tuffin, W. Sallem, J. C. Florent, *Bioorg. Med. Chem. Lett.* **2006**, *16*, 3147–3149.
[5] R. van Brakel, R. C. Vulders, R. J. Bokdam, H. Grüll, M. S. Robillard, *Bioconjugate Chem.* **2008**, *19*, 714–718.
[6] S. C. Alley, N. M. Okeley, P. D. Senter, *Curr. Opin. Chem. Biol.* **2010**, *14*, 529–537.
[7] R. Rossin, P. Renart-Verkerk, S. M. van den Bosch, R. C. M. Vulders, I. Verel, J. Lub, M. S. Robillard, *Angew. Chem.* **2010**, *122*, 3447–3450; *Angew. Chem. Int. Ed.* **2010**, *49*, 3375–3378.
[8] R. Rossin, S. M. van den Bosch, W. ten Hoeve, M. Carvelli, R. M. Versteegen, J. Lub, M. S. Robillard, *Bioconjugate Chem.* **2013**, *24*, 1210–1217.
[9] N. K. Devaraj, G. M. Thurber, E. J. Keliher, B. Marinelli, R. Weissleder, *Proc. Natl. Acad. Sci. USA* **2012**, *109*, 4762–4767.
[10] B. M. Zeglis, K. K. Sevak, T. Reiner, P. Mohindra, S. D. Carlin, P. Zanzonico, R. Weissleder, J. S. Lewis, *J. Nucl. Med.* **2013**, *54*, 1389–1396.
[11] B. Stanovnik, M. Tisler, A. R. Katritzky, O. V. Denisko, *Adv. Heterocycl. Chem.* **2001**, *81*, 254–303.
[12] J. Sauer, D. K. Heldmann, J. Hetzenegger, J. Krauthan, H. Sichert, J. Schuster, *Eur. J. Org. Chem.* **1998**, 2885–2896.
[13] M. T. Taylor, M. L. Blackman, O. Dmitrenko, J. M. Fox, *J. Am. Chem. Soc.* **2011**, *133*, 9646–9649.
[14] B. Rickborn in *Organic Reactions*, *Vol. 53* (Ed.: L. A. Paquette), Wiley, New York, **1998**, pp. 264–271, 523–576.
[15] A. Warnecke in *Drug Delivery in Oncology: From Basic Research to Cancer Therapy*, 1st ed. (Eds.: F. Kratz, P. Senter, H. Steinhagen), Wiley-VCH, Weinheim, **2011**, pp. 553–589.
[16] G. W. Ashley, J. Henise, R. Reid, D. V. Santi, *Proc. Natl. Acad. Sci. USA* **2013**, *110*, 2318–2323.
[17] M. Royzen, G. P. A. Yap, J. M. Fox, *J. Am. Chem. Soc.* **2008**, *130*, 3760–3761.
[18] G. H. Whitham, M. Wright, *J. Chem. Soc. C* **1971**, 883–896.
[19] L. Avellén, I. Crossland, *Acta Chem. Scand.* **1969**, *23*, 1887–1895.
[20] The reactivity between **3** and **8a-Bn** is only ca. 20-fold lower than that exploited successfully for pretargeting in mice in Ref. [7]. In an ADC application, the administration of **3** in excess, which is not possible in pretargeting, can compensate this lower reactivity.